

## A Novel Strategy for the Design of 8-Hydroxyquinolate-Based Lanthanide Bioprobes That Emit in the Near Infrared Range

Steve Comby, Daniel Imbert,\* Caroline Vandevyver, and Jean-Claude G. Bünzli<sup>[a]</sup>

**Abstract:** A new polydentate tripodal ligand **T2soxMe** was synthesized to take advantage of the chelating effect of tridentate 8-hydroxyquinolate subunits. Potentiometric and spectrophotometric titrations reveal seven  $pK_a$  values of between 3.7 and 10.2. In water, the use of **T2soxMe** leads to thermodynamically stable and soluble  $\text{Ln}^{\text{III}}$  complexes at physiological pH, with conditional stability constants in the range  $\log \beta_{11} = 7.8\text{--}8.6$ . The chelates are resistant toward hydrolysis and show interesting photophysical proper-

ties, particularly in the near infrared (NIR) range. The emission lifetimes of the  $\text{Nd}^{\text{III}}$  and  $\text{Yb}^{\text{III}}$  complexes recorded in  $\text{D}_2\text{O}$  and  $\text{H}_2\text{O}$  suggest the absence of water molecules in the first coordination sphere of the metal ions. Moreover, the low energy of the triplet state allows efficient energy transfer from the ligand to the metal ions: in water

at pH 7.4, the sensitization efficacy of the NIR luminescence reaches 75 and  $\approx 100\%$  for  $\text{Nd}^{\text{III}}$  and  $\text{Yb}^{\text{III}}$ , respectively, leading to overall quantum yields of 0.027 and 0.13%;  $\text{Er}^{\text{III}}$  luminescence is also detected. According to the WST-1 test, the  $\text{Yb}^{\text{III}}$  podate at concentrations of up to  $250 \mu\text{M}$  does not display sizeable cytotoxicity for Jurkat cells after 24 h of incubation. Finally, the same podate is shown to couple to human serum albumin, leading to an increase of 50% in the NIR-luminescence intensity.

**Keywords:** bioprobes • hydroxyquinoline • lanthanides • ligand effects • luminescence

### Introduction

The large degree of attention devoted presently to molecular compounds that emit in the near infrared (NIR) region originates from the requirements of medical diagnostics, cell imaging, and photonic materials, such as planar optical amplifiers or light-emitting diodes, for use in the telecommunications industry.<sup>[1–4]</sup> The intrinsic photophysical properties of trivalent lanthanide ions, narrow and easily recognizable emission lines, relatively long lifetimes of their excited states, and large Stokes' shifts upon excitation through indirect processes,<sup>[5]</sup> make them ideal candidates as emitting centers for these applications. Trivalent lanthanides are hard spherical ions without stereochemical preferences and, therefore, their specific insertion into stable and kinetically inert environments, a requirement for efficient luminescent probes, necessitates carefully planned strategies.<sup>[6–8]</sup> Among

them, the induced-fit concept,<sup>[9]</sup> sometimes combined with the use of self-assembly processes,<sup>[6,7]</sup> has proven to be successful in the tailoring of adequate receptors. However, chemical requirements are not the only constraints in the design of efficient lanthanide-based luminescent probes: photophysical aspects must be taken into account, and these can be summarized simply as follows. Firstly, because f–f transitions have low oscillator strengths due to their forbidden nature, excitation of the luminescent centers relies on energy transfer from their environment. In molecular compounds, an important path involves the triplet state of the ligand(s), so that the coordinated ligand should have high intersystem-crossing efficiency, in addition to a triplet-state energy  $E(^3\pi\pi^*)$  close to, but larger than, the emissive excited state of the metal ion. Energy transfer from the ligand singlet state is also feasible, particularly for  $\text{Nd}^{\text{III}}$ , but is usually less efficient. For  $\text{Yb}^{\text{III}}$ , which, contrary to most other lanthanide ions, possesses only two electronic levels, the situation is more complex and either phonon-assisted transfer from the triplet state (or metal-to-ligand charge-transfer states) or an internal double-electron transfer mechanism account for the population of its  $^2\text{F}_{5/2}$  fluorescent state.<sup>[10,11]</sup> Secondly, the metal ion environment must be rigid enough and devoid of high-energy oscillators to avoid de-excitation through vibrational processes. In the case of NIR-emitting

[a] S. Comby, Dr. D. Imbert, Dr. C. Vandevyver, Prof. Dr. J.-C. G. Bünzli  
Laboratory of Lanthanide Supramolecular Chemistry  
École Polytechnique Fédérale de Lausanne (EPFL)  
BCH 1402, 1015 Lausanne (Switzerland)  
Fax: (+41) 21-693-9825  
E-mail: Daniel.Imbert@epfl.ch

Supporting information for this article is available on the WWW under <http://www.chemeurj.org/> or from the author.

ions, such as Nd<sup>III</sup>, Er<sup>III</sup>, and Yb<sup>III</sup>, the presence of high-energy oscillators (C–H, N–H, O–H) in the ligand(s), although outside the inner coordination sphere, leads to dramatic extinction of the luminescence. As a consequence, the overall quantum yield  $Q_{Ln}^L$ , obtained by excitation in the ligand levels, remains very small, particularly in water, usually <0.1% for Nd<sup>III</sup>, <0.001% for Er<sup>III</sup>, and <0.1% for Yb<sup>III</sup>. Indeed, this parameter is linked to the sensitization efficacy of the ligand,  $\eta_{sens}$ , and the intrinsic quantum yield  $Q_{Ln}^{Ln}$ , determined upon direct excitation in the Ln<sup>III</sup> levels and which consequently reflects the deactivation processes:

$$Q_{Ln}^L = \eta_{sens} \cdot Q_{Ln}^{Ln}$$

The sensitization efficacy of the ligand is well established, with  $\eta_{sens}$  commonly much larger than 50%, as we have recently shown with an appended terpyridine–boradiazaindene dye used both as chelating and sensitizing unit.<sup>[12]</sup> This is not yet the case for the deactivation processes, particularly for the luminescent ions that have a small energy gap between the emitting level and the next electronic level of lower energy, unless substantial modifications of the ligand, such as deuteration or fluorination, are performed.<sup>[3]</sup>

However, by taking into account the fact that Yb<sup>III</sup> appears to be the lanthanide ion best adapted for biomedical applications, we recently showed that **TsoxMe**, a tetrapodal ligand featuring bidentate 7-carboxy-8-hydroxyquinolate coordinating units, meets both the chemical (pLn=15–16) and photophysical ( $\eta_{sens} \approx 70$ –100% for Nd<sup>III</sup> and Yb<sup>III</sup>) requirements for a NIR-emitting luminescent probe, with a quantum yield of up to 0.37% in water for Yb<sup>III</sup>.<sup>[13]</sup> Here, we tested a novel strategy based on the same chromophore, but in which the chromophore was connected by its 2-position, which renders it tridentate, and to a smaller framework, namely tris(ethylamine) rather than *N,N*-bis(propyl)ethylenediamine. In addition to the thermodynamic and photophysical studies of the resulting podates (Ln = Pr, Nd, Gd, Er, Yb) in water, we also tested the cytotoxicity of the Yb<sup>III</sup> chelate, as well as its ability to couple with human serum albumin (HSA).

## Results and Discussion

Ligand **T2soxMe** was obtained according to the synthetic pathway depicted in Scheme 1. The starting triamine is a commercial product and was methylated as previously described.<sup>[14]</sup> In the next step, this product was condensed with activated 2-carboxy-8-hydroxyquinoline to give the tripodal ligand **T2oxMe**. Finally, the regioselective sulfonation of the 8-hy-

droxyquinoline subunits was achieved by using oleum (H<sub>2</sub>SO<sub>4</sub>, SO<sub>3</sub>), as already reported for 2-carboxy-8-hydroxyquinoline,<sup>[15]</sup> giving an overall yield of 27%.

### Solution study: thermodynamic aspects

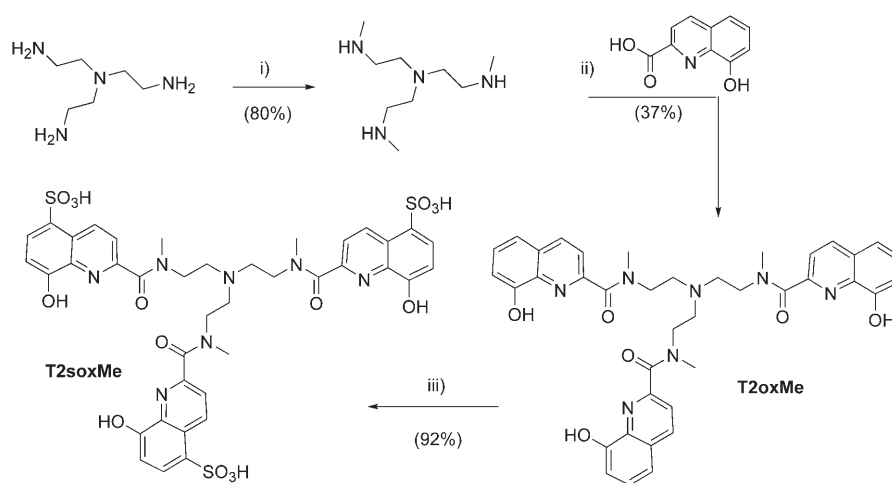
**Ligand deprotonation constants:** The fully protonated **T2soxMe** ligand, denoted (H<sub>10</sub>L)<sup>4+</sup>, possesses ten deprotonation sites, three pyridinium groups, and one tertiary nitrogen atom, three hydroxyl oxygen atoms, and three sulfonate groups. The three sulfonate groups are totally deprotonated under the conditions used; the starting species is generally denoted (H<sub>7</sub>L)<sup>+</sup> in this paper. The deprotonation constants were determined separately by potentiometry and spectrophotometry. The extracted p*K*<sub>ai</sub> values obtained by titrations in the 1.5–12.5 pH range are defined by Equations (1) and (2):

$$H_{8-i}L^{(2-i)+} \rightleftharpoons H_{7-i}L^{(1-i)+} + H^+ \quad (1)$$

$$K_{ai} = [H_{7-i}L^{(1-i)}] \cdot [H^+] / [H_{8-i}L^{(2-i)+}] \quad (2)$$

The potentiometric titration of the protonated form (H<sub>7</sub>L)<sup>+</sup> of the ligand with NaOH in 0.1 M KCl at 25 °C (see Supporting Information, Figure S1) allowed the determination of four deprotonation constants. Analysis of the potentiometric titration curve over the pH range 2.5–12.26 gave four p*K*<sub>ai</sub> values (Table 1), defined by Equations (1) and (2).

Spectrophotometric titration carried out in the pH range 1.04–12.99 at lower concentration (Figure 1) allowed us to 1) establish the p*K*<sub>a</sub> values that could not be determined by potentiometry, and 2) confirm the values already obtained in the higher-pH range. The absorption spectra (Figure 1a) show the presence of several isobestic points at 253, 254, 263, 297, 329, 334, and 410 nm. The best refinement allowed us to determine all the p*K*<sub>a</sub> values, except for p*K*<sub>a3</sub> and p*K*<sub>a4</sub>, for which only the sum could be calculated (Table 1). The calculated spectra (Figure 1b) are in good agreement with



Scheme 1. Synthetic pathway used to obtain ligand **T2soxMe**: i) a) EtCO<sub>2</sub>Cl, H<sub>2</sub>O, toluene; b) LiAlH<sub>4</sub>, THF; ii) 2-carboxy-8-hydroxyquinoline, *N,N*-carbonyl diimidazole (CDI), THF; iii) H<sub>2</sub>SO<sub>4</sub>, SO<sub>3</sub> (20%).

Table 1. Deprotonation constants of  $(H_7L)^+$  ( $\pm\sigma$ , see Equations (1) and (2) for the definition of  $K_{a_i}$ ).

|                     | [a]      | [b]      | $\log \beta_{10}^{[a,b]}$ |
|---------------------|----------|----------|---------------------------|
| $pK_{a1}$           | –        | 3.7(1)   | 47.0(1)                   |
| $pK_{a2}$           | –        | 4.62(7)  | 43.29(7)                  |
| $pK_{a3} + pK_{a4}$ | –        | 11.41(6) | 38.67(6)                  |
| $pK_{a4}$           | 6.85(9)  | –        | 34.11(9)                  |
| $pK_{a5}$           | 8.33 (9) | 7.88(6)  | 27.26(9)                  |
| $pK_{a6}$           | 8.70(9)  | 9.01(5)  | 18.93(9)                  |
| $pK_{a7}$           | 10.23(8) | 10.05(3) | 10.23(8)                  |

[a] Potentiometric data:  $[L]_0 = 5.98 \cdot 10^{-4} \text{ M}$ ;  $\mu = 0.1 \text{ M}$  (KCl);  $T = 25^\circ \text{ C}$ .  
[b] Spectrophotometric data:  $[L]_0 = 6.5 \cdot 10^{-6} \text{ M}$ ;  $\mu = 0.1 \text{ M}$  (KCl);  $T = 25.0^\circ \text{ C}$ .

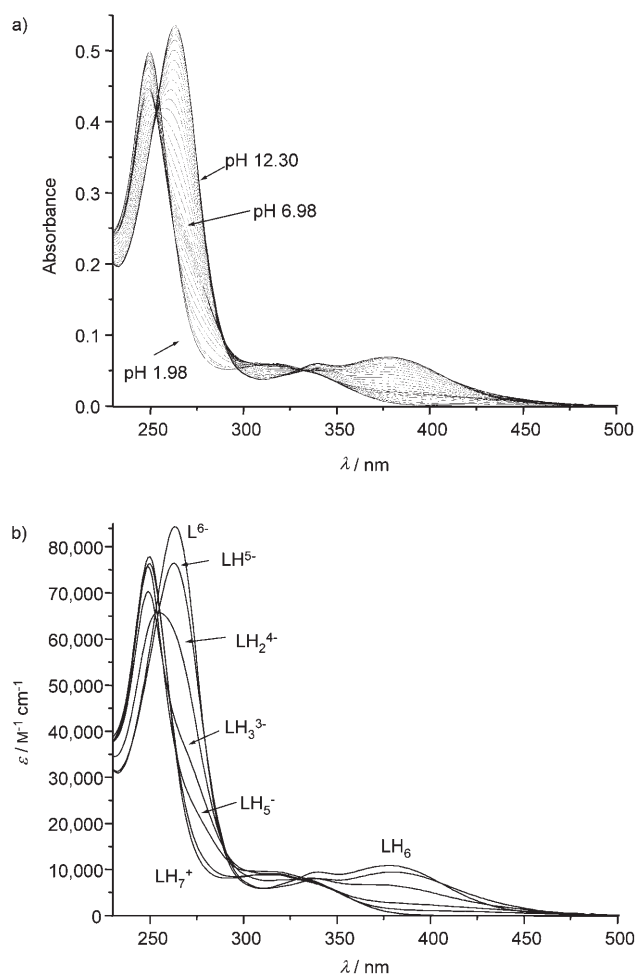


Figure 1. a) UV/Vis absorption spectra of  $(H_7L)^+$  as a function of pH in water:  $[T2soxMe] = 6.5 \cdot 10^{-6} \text{ M}$ ;  $T = 25.0 \pm 0.1^\circ \text{ C}$ ;  $\mu = 0.1 \text{ M}$  (KCl). b) Recalculated spectra of the various species.

the experimental data. Extractions at different wavelengths are presented in the Supporting Information, Figure S1.

The three lowest  $pK_a$  values are attributed to the pyridinium nitrogen atoms by comparison with the  $pK_a$  values of O-Trensox (1.83, 2.55, and 3.01),<sup>[16]</sup> a tripodal ligand based on sulfonated 7-carboxy-8-hydroxyquinoline, and with the value of 3.92 published for 5-sulfo-8-hydroxyquinoline.<sup>[17]</sup> In our

case, four  $pK_a$  values are between 6.85 and 10.23, the first being attributed to the central nitrogen as it is close to the value reported for O-Trensox. The three other dissociation constants have an average of 9.09 and are due to the hydroxyl moieties. The corresponding values for O-Trensox are between 7.44 and 8.62 with an average of 8.07, whereas that for 5-sulfo-8-hydroxyquinoline is 8.42. This difference can be attributed to the position of the carboxylation in **T2soxMe**, position two instead of position seven in the case of O-Trensox and, moreover, the three  $pK_a$  values differ from the statistical factor of  $\log 3 = 0.48$  (the value for noninteracting arms). In contrast to the situation for O-Trensox, this indicates cooperativity between the arms of the tripodal ligand, which is probably due to the presence of the methyl groups and of intra- or intermolecular hydrogen bonds. The corresponding distribution curves are presented in Figure 2.

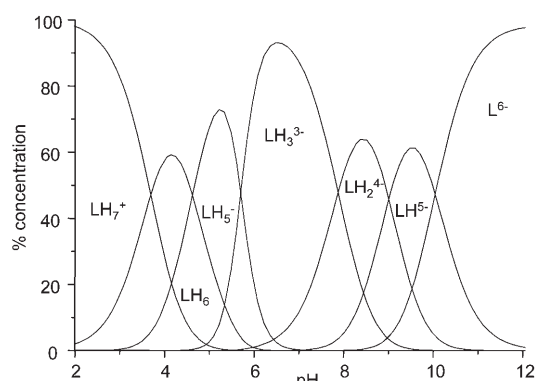
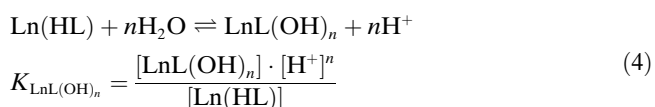
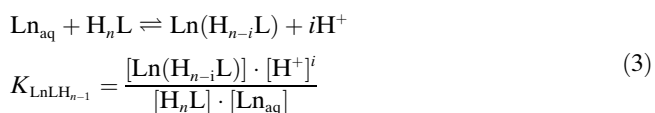


Figure 2. Distribution curves of the ligand computed from the  $pK_a$  values at pH 2–12.

*Interaction with trivalent lanthanide ions:* To unravel the influence of pH on the speciation, the equilibria of the different metal complexes present in solution were studied by performing potentiometric and spectrophotometric titrations. The potentiometric titration curve of a 1:1 solution of  $Yb^{III}$  and **T2soxMe** did not enable us to determine the global constants defined by Equations (3) and (4), in spite of several models tested to refine the titration data:



Despite the complexity of the system, it is clear from the spectrophotometric data that at physiological pH only one major species is present. The stability of this species appears to be comparable to the one determined for the tetrapodal

complexes with **TsoxMe** (e.g.,  $pEu=14.9^{[13]}$ ). For instance, the addition of two equivalents of the tetrapodal ligand leads to partial decomplexation of  $[Ln-T2soxMe]$  only. On the other hand, the addition of one equivalent of diethylenetriaminopentaacetic acid (DTPA) ( $pEu=19.6$  computed from known stability constants<sup>[17]</sup>) results in a large dissociation of the  $Eu^{III}$  tripodal chelate. Therefore, we estimate that the  $pEu$  value for the **T2soxMe** chelate is between 15 and 19, and the corresponding values for the other lanthanide ions studied here should be similar, referring to the range of values obtained for **TsoxMe** (15–16).

Next, the interaction between  $Ln^{III}$  ions ( $Ln = Nd, Gd, Dy, Yb$ ) and the ligand was monitored by UV-visible spectrophotometry (Figure 3) by using dilute aqueous solutions

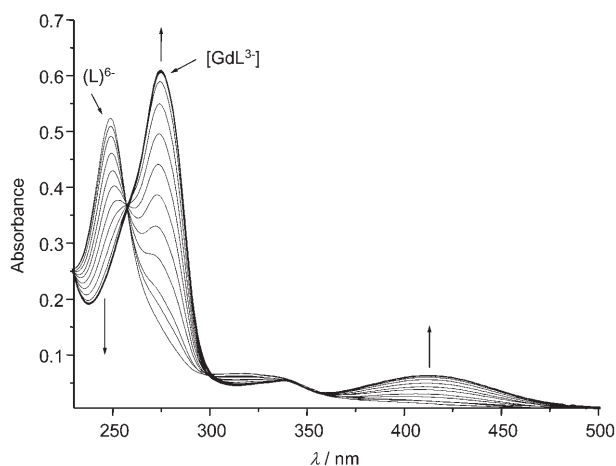


Figure 3. Evolution of the UV/Vis absorption spectra of a solution of **T2soxMe** in buffered water (pH 7.4, HBS) upon addition of increasing amounts of  $Gd^{III}$ .

at pH 7.4 in Hepes-buffered saline (HBS buffer). The variation in absorbance versus  $R = [Ln^{III}]_{tot}/[L]_{tot}$  indicates the presence of one species, the 1:1 complex, in the stoichiometry range investigated ( $0 < R < 4$ ) for which  $[L]_0 = 6.5 \cdot 10^{-6}$  M, pH 7.4, and  $T = 25.0^\circ C$  ( $20.0^\circ C$  for  $Yb^{III}$ ). The conditional stability constants extracted from these data are  $\log \beta_{11} = 8.2(5), 8.5(7), 8.6(6), 7.8(2)$  for  $Ln = Nd, Gd, Dy,$  and  $Yb$ , respectively.

The complexation of **T2soxMe** with  $Pr^{III}, Nd^{III},$  and  $Lu^{III}$  was also investigated by conducting  $^1H$  NMR experiments in which the spectra of the ligands ( $10^{-3}$  M in  $D_2O$ ) were monitored as a function of aliquots of cations added, the pD being fixed at 7.5 by using Tris-DCl buffer (0.1 M). For diamagnetic lutetium (Figure S2, Supporting Information), a rapid evolution was observed during the addition of  $Lu^{III}$ , until 0.8 equivalents of metal had been added. Further additions did not result in an observable spectral change. Clearly, only one species is formed, with a stoichiometric ratio of 1:1. For  $Ln:L$  ratios larger than 1, the peaks remained identical and a new one appeared at 9.15 ppm after addition of between 1.5–3 equivalents of  $Lu^{III}$ . This could indicate the possible formation of polynuclear species that were not ob-

served during UV-visible titration experiments because the concentrations were too low. The same evolution was observed for the signals in the aliphatic part of the NMR spectra. Other titration experiments with the paramagnetic praseodymium cation gave similar results (Figure 4). In addition, one signal is present for each proton of the 8-hydroxyquinoline subunit, indicating that the three arms are coordinated to the lanthanide ion and, thus, are equivalent on the NMR timescale.

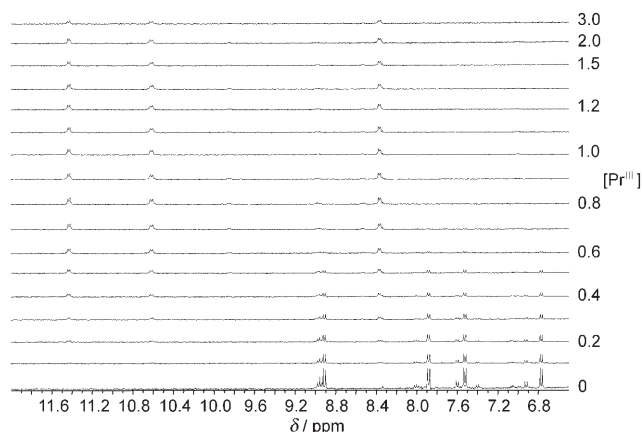


Figure 4. Evolution of the  $^1H$  NMR spectra of **T2soxMe** in buffered  $D_2O$  (Tris-DCl, pD 7.5) as a function of added  $Pr^{III}$ .

**Photophysical properties of T2soxMe:** In water, the absorption spectra of the ligand features two main bands (with additional shoulders) located at around  $38000$  and  $26500$   $cm^{-1}$  and assigned to  $\pi \rightarrow \pi^*$  and  $n \rightarrow \pi^*$  transitions. The high-energy band is blue-shifted by  $1400$   $cm^{-1}$  in progressing from the acidic to the basic forms of the ligand. The low-energy absorption appears to be more sensitive to the deprotonation process of **T2soxMe** (a shift of  $5000$   $cm^{-1}$ ). Under excitation at these wavelengths, an emission band appears, centered at  $19000$   $cm^{-1}$ , which disappears upon enforcement of a time delay and is consequently assigned as arising from a  $^1\pi\pi^*$  state. At low temperature ( $77$  K, in solutions containing 10% glycerol), a second emission band appears in the range  $16500$ – $17500$   $cm^{-1}$ , corresponding to phosphorescence from the triplet state(s). The ligand-centered luminescence spectra of the 1:1 complexes with  $La^{III}, Eu^{III}, Gd^{III},$  and  $Lu^{III}$ , both at room temperature in aqueous solutions and at  $77$  K in a frozen water/glycerol mixture, have essentially the same features, with slight shifts of the maxima (Figure 5). The phosphorescence decays are mono-exponential functions, with associated lifetimes of  $29(1), 0.51(2),$  and  $21.5(5)$  ms for the complexes of  $La^{III}, Gd^{III},$  and  $Lu^{III}$ , respectively. In the case of the  $Eu^{III}$  complex, the  $^3\pi\pi^*$  emission is not detected, and the characteristic emission lines of the metal ion are observed, reflecting a complete  $^3\pi\pi^* \rightarrow Eu^{III}$  transfer at low temperature. At room temperature, the  $Eu^{III}$  luminescence is not observable, due to the energy gap  $\Delta E(^3\pi\pi^* \rightarrow ^5D_0)$  being too small and allowing efficient back-transfer onto the ligand.

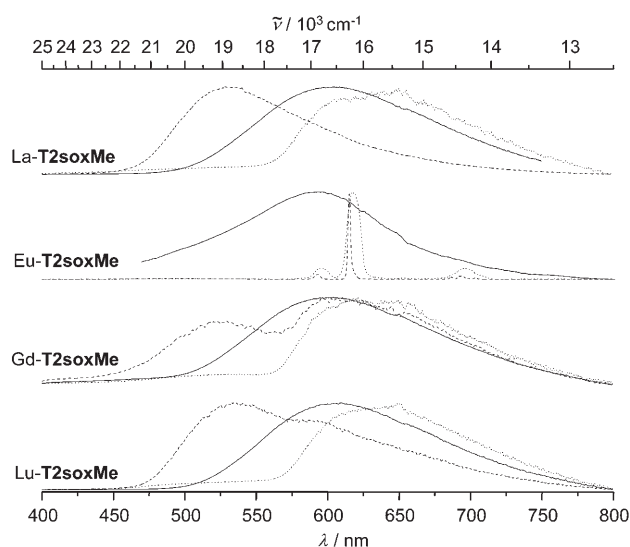


Figure 5. Luminescence spectra of **T2soxMe** and its 1:1 complexes at 77 K in  $6 \cdot 10^{-5}$  M in HBS buffer pH 7.4 containing 10% glycerol, without (---) and with (.....) a 0.05 ms time delay, and at RT (—).

**Sensitization of lanthanide-centered NIR emission by T2soxMe:** All the chelates with  $\text{Nd}^{\text{III}}$ ,  $\text{Er}^{\text{III}}$ , and  $\text{Yb}^{\text{III}}$  display metal-centered NIR luminescence in aqueous solutions at physiological pH. Moreover, the ligand luminescence almost disappears, with only a faint emission from the singlet state ( $\approx 5\text{--}10\%$  compared with the free ligand), which indicates an efficient energy-transfer process from the ligand levels to the acceptor levels of the metal ions. At room temperature and upon broad band excitation through the ligand levels both at 274 ( $36500\text{ cm}^{-1}$ ) and 417 nm ( $23980\text{ cm}^{-1}$ ), the luminescence spectra display the peaks corresponding to the expected transitions. The  $\text{Yb}^{\text{III}}$  complex emits in the 920–1100 nm range, with a sharp band at 977 nm assigned to the  ${}^2\text{F}_{5/2} \rightarrow {}^2\text{F}_{7/2}$  transition and a broader vibronic component<sup>[18]</sup> at longer wavelength. Under the same conditions, the  $\text{Nd}^{\text{III}}$  complex displays NIR luminescence in the 840–1430 nm range, the main band being centered at 1064 nm. The three bands occur in the ranges 840–940, 1020–1135, and 1290–1370 nm, and are assigned to transitions from the  ${}^4\text{F}_{3/2}$  level to the  ${}^4\text{I}_{9/2}$ ,  ${}^4\text{I}_{11/2}$ , and  ${}^4\text{I}_{13/2}$  sublevels, respectively. Finally, the luminescence spectrum of the  $\text{Er}^{\text{III}}$  complex in solution was recorded, displaying the typical  ${}^4\text{I}_{13/2} \rightarrow {}^4\text{I}_{15/2}$  transition centered at 1540 nm. If water is replaced by deuterated water, the shape of the luminescence spectra remains unchanged, as expected, but the overall intensity increases considerably. The close similarity in the absorption and excitation spectra (Figure 6, left) of the three lanthanide chelates ( $\text{Nd}^{\text{III}}$ ,  $\text{Er}^{\text{III}}$ , and  $\text{Yb}^{\text{III}}$ ) clearly indicates sensitization of the NIR luminescence by the ligand.

Furthermore, we determined the lifetimes (Table 2) of the  $\text{Nd}({}^4\text{F}_{3/2})$ ,  $\text{Er}({}^4\text{I}_{13/2})$ , and  $\text{Yb}({}^2\text{F}_{5/2})$  excited states upon excitation by using the Nd:YAG line at 355 nm. The luminescence decays are all monoexponential and the corresponding lifetimes in water are 0.15(1), 0.24(1), and 2.47(1)  $\mu\text{s}$  for  $\text{Nd}^{\text{III}}$ ,  $\text{Er}^{\text{III}}$ , and  $\text{Yb}^{\text{III}}$ , respectively. These lifetimes are appreciably

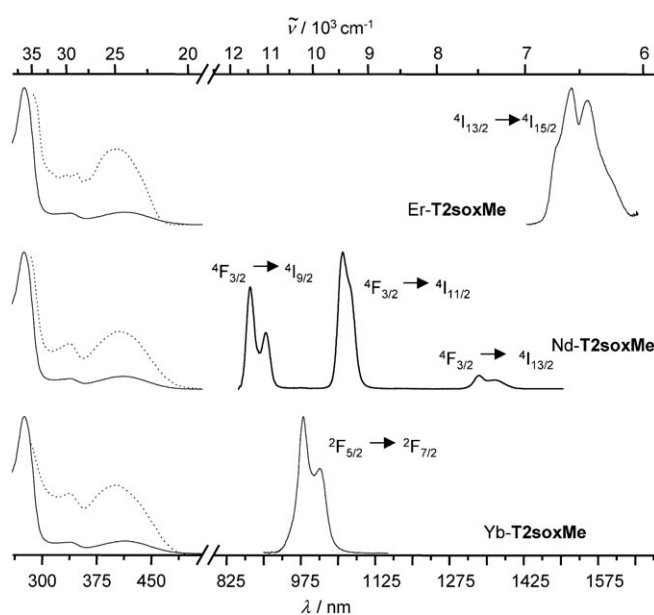


Figure 6. Left: Normalized absorption and excitation spectra (.....,  $\lambda_{\text{an}} = 1540$  (Er), 1063 (Nd), and 976 nm (Yb)). Right: Emission spectra in the NIR region ( $\lambda_{\text{ex}} = 417$  nm) of the 1:1 chelates of  $\text{Er}^{\text{III}}$ ,  $\text{Nd}^{\text{III}}$ , and  $\text{Yb}^{\text{III}}$ . All solutions were in water at pH 7.4 and RT.

Table 2. Metal-ion-centered lifetimes ( $\tau$ ) for  $\text{Nd}({}^4\text{F}_{3/2})$ ,  $\text{Er}({}^4\text{I}_{13/2})$ , and  $\text{Yb}({}^2\text{F}_{5/2})$  in the Ln-**T2soxMe** podates at pH 7.4 (HBS buffer) in water and  $\text{D}_2\text{O}$  solution, absolute quantum yields ( $Q$ , relative uncertainty  $\pm 20\%$ ), and number of water molecules bound in the inner coordination sphere ( $q$ ).

| Ln <sup>[a]</sup> | $\lambda_{\text{an}}$ [nm <sup>-1</sup> ] | $\tau$ [ $\mu\text{s}$ ] |                      | $Q_{\text{Ln}}^{\text{L}}$ [%] |                      | $q^{\text{[b]}}$ |
|-------------------|---|--------------------------|----------------------|--------------------------------|----------------------|------------------|
|                   |   | $\text{H}_2\text{O}$     | $\text{D}_2\text{O}$ | $\text{H}_2\text{O}$           | $\text{D}_2\text{O}$ |                  |
| Nd                | 1063                                      | 0.15(2)                  | 0.91(4)              | 0.027(5)                       | 0.075(15)            | 0.31             |
| Er                | 1540                                      | 0.24(2)                  | 2.55(2)              | –                              | $3.5 \cdot 10^{-3}$  | –                |
| Yb                | 976                                       | 2.47(6)                  | 26.6(6)              | 0.13(3)                        | 1.5(3)               | 0.16             |

[a]  $[\text{Ln-T2soxMe}] = 6.5 \cdot 10^{-5}$  M (Ln = Er, Yb, Nd). [b] From Equations (5) and (6); see text for uncertainties.

longer in deuterated water. The former lifetimes are in line with those published for polycarboxylate complexes derived from DTPA,<sup>[19]</sup> 0.58, 1.46, and 10.4  $\mu\text{s}$  for  $\text{Nd}^{\text{III}}$ ,  $\text{Er}^{\text{III}}$ , and  $\text{Yb}^{\text{III}}$ , respectively, and more recently, from the ligand **TsoxMe**: 0.61(1), 2.31(2), and 14.6(1)  $\mu\text{s}$  for  $\text{Nd}^{\text{III}}$ ,  $\text{Er}^{\text{III}}$ , and  $\text{Yb}^{\text{III}}$ , respectively.<sup>[13]</sup>

The number of bound water molecules around the metal ions in the Ln-**T2soxMe** podates with  $\text{Nd}^{\text{III}}$  and  $\text{Yb}^{\text{III}}$  was determined by using Equations (5) and (6), proposed by Faulkner and co-workers<sup>[20,21]</sup> for  $\text{Nd}^{\text{III}}$  aminocarboxylates ( $q=0\text{--}2$ ), and by Beeby and co-workers<sup>[22]</sup> for  $\text{Yb}^{\text{III}}$  complexes ( $q \leq 1$ ):

$$q = A(\Delta k_{\text{obs}}) - C \text{ for } \text{Nd}^{\text{III}} \quad (5)$$

$$q = A(\Delta k_{\text{obs}} - B) \text{ for } \text{Yb}^{\text{III}} \quad (6)$$

in which  $A = 130$  ns ( $\text{Nd}^{\text{III}}$ ) or 1  $\mu\text{s}$  ( $\text{Yb}^{\text{III}}$ ),  $B = 0.2\text{ }\mu\text{s}^{-1}$ , and  $C = 0.4$ ;  $\Delta k_{\text{obs}}$  is given in  $\text{ns}^{-1}$  and  $\mu\text{s}^{-1}$  for  $\text{Nd}^{\text{III}}$  and  $\text{Yb}^{\text{III}}$ , re-

spectively,  $k_{\text{obs}} = 1/\tau_{\text{obs}}$  and  $\Delta k_{\text{obs}} = k_{\text{obs}}(\text{H}_2\text{O}) - k_{\text{obs}}(\text{D}_2\text{O})$ . By using these Equations, we obtain  $q = 0.31$  and  $0.16$  for  $\text{Nd}^{\text{III}}$  and  $\text{Yb}^{\text{III}}$ , respectively. These values are much smaller than unity, indicating complexes with no coordinated water molecules around the metal ion. This is in line with a complete coordination of the three pendant arms of the podand that acts consequently as a nonadentate host. Indeed, given the uncertainty of  $q$  ( $\pm 0.1$ – $0.3$ ), we do not think that the residual values reflect equilibria involving hydrated species, but, rather, that they arise from second-sphere effects not taken into account by parameters  $B$  and  $C$ .

To quantify the ability of the chromophoric subunits of **T2soxMe** to sensitize the NIR-emitting lanthanides, the absolute quantum yields of the  $\text{Ln-T2soxMe}$  podates ( $\text{Ln} = \text{Nd}, \text{Er}, \text{Yb}$ ) were determined in aqueous solutions upon ligand excitation. Under the experimental conditions used ( $6.5 \cdot 10^{-5} \text{ M}$  HBS-buffered solutions, pH 7.4), the quantum yields are 0.027 and 0.13% for  $\text{Nd}^{\text{III}}$  and  $\text{Yb}^{\text{III}}$ , respectively, and these increase by 2.8- and 11.5-fold in deuterated water, respectively.  $\text{Er}^{\text{III}}$  luminescence in water is too weak for a quantum yield to be determined, however, the corresponding value could be measured in  $\text{D}_2\text{O}$ . These quantum yields are large relative to published data and are of the same order of magnitude to those reported for **TsoxMe**,<sup>[13]</sup> particularly for  $\text{Yb}^{\text{III}}$  and for aqueous solutions in which the presence of proximate OH vibrations in the second coordination sphere induces a large quenching effect for the ions that have a small energy gap. If we use, as a first approximation, the radiative lifetimes of 0.42 and 2 ms for  $\text{Nd}^{\text{III}}$  and  $\text{Yb}^{\text{III}}$  corresponding to the aquo ions,<sup>[13]</sup> we find that  $\eta_{\text{sens}} = Q_{\text{Ln}}^{\text{L}} / Q_{\text{Ln}}^{\text{Ln}} \approx 75$  and 100% for the ligand sensitization efficacy in the  $\text{Nd}^{\text{III}}$  and  $\text{Yb}^{\text{III}}$  chelates, respectively. That is, the modest overall quantum yields are essentially due to deactivation processes involving vibrational oscillators located outside the first coordination sphere.

**Cytotoxicity and interaction with HSA:** To quantify the influence of the  $\text{Yb-T2soxMe}$  complex on the viability of the cells, the WST-1 test was used. To determine the optimal incubation time, a preliminary experiment was performed by taking measurements after 0.5, 1, 2, 3.5, and 4.5 h (Figure S3, Supporting Information). An increase in absorbance (450–650 nm) is observed over time, reflecting the proliferation of the cells (Figure S4, Supporting Information). However, for concentrations of  $\text{Yb-T2soxMe}$  complex  $> 125 \mu\text{M}$ , a negative influence on cell proliferation is observed and is confirmed by measurements after 24 h. Compared to the cells not incubated with the complex, there is no significant change in cell viability for concentrations up to  $125 \mu\text{M}$ . However, the viability drops to 90% for  $250 \mu\text{M}$  and to 70% for  $500 \mu\text{M}$  (Figure 7), indicative of a toxic effect occurring at only high concentrations of the  $\text{Yb-T2soxMe}$  chelate.

Finally, we measured the luminescence intensity and the lifetimes of the  $\text{Yb-T2soxMe}$  complex in a buffered medium containing different quantities of HSA, from 0 to 100 equivalents with respect to the complex, as reported previously.<sup>[23]</sup> The luminescence increased by 50% upon addition of the

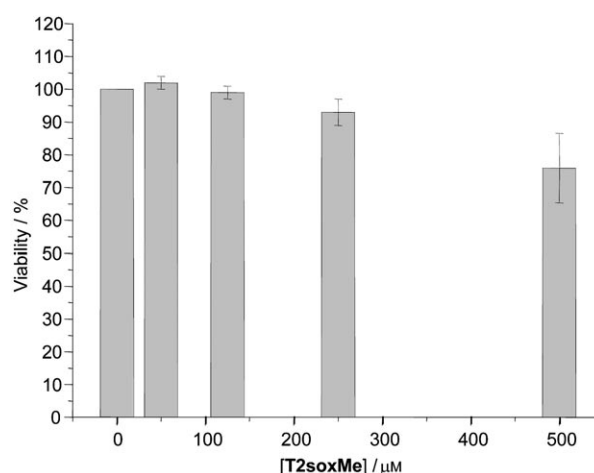


Figure 7. Cell viability values (%) obtained by using the WST-1 test of Jurkat cells for different concentrations of the  $\text{Yb-T2soxMe}$  complex after 24 h incubation.

first equivalent of HSA and remained constant upon further additions. This indicates that addition of this protein to the medium does not quench the luminescence of the complex, but rather, that interaction between the complex and the protein takes place, resulting in an increase in luminescence intensity. On the other hand, the lifetime of the  $\text{Yb}^{\text{III}}$  level does not change significantly in response to HSA addition (between 2.47 and 2.52  $\mu\text{s}$  for 0.1–100 equivalents of HSA).

## Conclusion

The tripodal ligand proposed here perfectly meets the chemical requirements for the design of an in vitro luminescent probe in that it wraps around the  $\text{Ln}^{\text{III}}$  ions, yielding hydrolysis-resistant, stable podates at physiological pH. The podand acts as a nonadentate receptor, as demonstrated by the equivalence of the three arms in the NMR spectra and by the absence of water molecules in the inner coordination sphere. Thus, one of the main deactivation paths of the  $\text{Ln}^{\text{III}}$  NIR luminescence is avoided.<sup>[3]</sup> Relative to our previous approach using **TsoxMe**, a tetrapodal ligand fitted with bidentate coordinating pendant arms,<sup>[13]</sup> the present strategy making use of a tris(tridentate) tripodal ligand is to some extent easier with respect to ligand synthesis and it yields chelates with similar stability. This strategy could be extended easily to the design of similar podates featuring a carbon anchor offering various derivatization possibilities. On the other hand, the photophysical properties are not as good, as exemplified by the shorter lifetimes of the tripodal derivatives relative to the tetrapodal chelates. In fact, the photophysical parameters are comparable to those obtained for the chelates with **Tsox**, the unmethylated analogue of **TsoxMe**, that is, they are still better than the ones reported for most of the complexes published to date.<sup>[3]</sup> The  $\text{Yb}^{\text{III}}$  podate appears to be particularly promising as its cytotoxicity is low (Jurkat cells, 24 h incubation,  $> 90\%$  cell viability

at concentrations  $< 250 \mu\text{M}$ ), and because it couples to HSA with a concomitant increase in luminescence intensity. This opens real perspectives for the development of bioprobes based on this system. Indeed, improvement of the photo-physical properties by taking advantage of the heavy-atom effect of the bromine substituents<sup>[24]</sup> on the 8-hydroxyquinoline moiety is within reach. Furthermore, proximate C–H vibrators could be removed by substitution with fluorine. These improvements are in progress in our laboratory and we are also working towards the development of a cell-imaging system based on this and other<sup>[13]</sup> Yb<sup>III</sup> luminescent stains.

## Experimental Section

Tetrahydrofuran (THF,  $> 99\%$ ) from Acros and methanol (99.9%) from Merck were purified by usual methods.<sup>[25]</sup> <sup>1</sup>H and <sup>13</sup>C NMR spectroscopy was performed by using a Bruker Avance DRX 400 spectrometer at 25°C, with deuterated solvents [D<sub>1</sub>]CHCl<sub>3</sub> and [D<sub>6</sub>]DMSO (dimethyl sulfide, 99.8 atom% D) from Armar Chemicals, and deuterium oxide (99.9 atom% D) from Aldrich as internal standards. Mid-infrared spectra were recorded by using a Perkin–Elmer Spectrum One spectrometer equipped with a Universal Attenuated Total Reflection sampler. ESI-MS spectra were obtained by using a Finnigan SSQ 710C spectrometer with  $10^{-4}$ – $10^{-5}$  M solutions in acetonitrile/H<sub>2</sub>O/acetic acid (50:50:1) or MeOH, a capillary temperature of 200°C, and an acceleration potential of 4.5 keV. This instrument was calibrated by using horse myoglobin and all analyses were conducted in the positive mode; the ion-spray voltage was 4.6 keV. The samples were introduced through a syringe pump operating at 20  $\mu\text{L min}^{-1}$ . Elemental analyses were performed by Dr. H. Eder from the Microanalytical Laboratory of the University of Geneva.

**Podand T2oxMe:** 2-Carboxy-8-hydroxyquinoline (1 g, 5.3 mmol) was dissolved in 100 mL of freshly distilled THF. A solution of *N*-hydroxysuccinimide (0.66 g, 5.7 mmol) and 1,3-dicyclohexylcarbodiimide (1.16 g, 5.7 mmol) in THF (50 mL) was added to the stirred solution. After 48 h of stirring at RT, a solution of compound **1** (0.25 g, 1.7 mmol) in dry THF (50 mL) was added within 60 min. The mixture was stirred for an additional 72 h and evaporated. The resulting residue was dissolved in chloroform (250 mL), successively washed with saturated NH<sub>4</sub>Cl, brine, and water (4  $\times$  250 mL), dried with MgSO<sub>4</sub>, and then evaporated to dryness. The residue was applied three times to a Sephadex LH-20 column (50% MeOH/CH<sub>2</sub>Cl<sub>2</sub>). An orange foam **3**, eluted as a single band, was obtained (445 mg, 37%). <sup>1</sup>H NMR (400 MHz, [D<sub>6</sub>]DMSO):  $\delta$  = 2.87 (t, 6H; CH<sub>2</sub>), 2.91 (s, 9H; CH<sub>3</sub>), 3.75 (m, 6H; CH<sub>2</sub>), 7.26 (d, 3H; ArH), 7.44 (d, 3H; ArH), 7.65 (t, 3H; ArH), 8.24 (d, 3H; ArH), 8.36 (d, 3H; ArH), 8.45 ppm (t, 3H; NH); IR (ATR):  $\tilde{\nu}$  = 3450–3230, 1616, 1453 cm<sup>-1</sup>; ESI-MS: *m/z*: calcd [M+H]<sup>+</sup>: 701.30; found: 702.35; calcd [M+2H]<sup>2+</sup>: 351.65; found: 351.85; elemental analysis calcd (%) for C<sub>39</sub>H<sub>39</sub>N<sub>7</sub>O<sub>6</sub>·MeOH: C 65.47, H 5.91, N 13.36; found: C 65.12, H 5.87, N 13.28.

**Podand T2soxMe: T2oxMe** (430 mg, 0.613 mmol) was placed in a round-bottomed flask and was covered with a minimum of oleum (H<sub>2</sub>SO<sub>4</sub>, SO<sub>3</sub>, 30%). The mixture was stirred at RT overnight and then poured onto ice, yielding a precipitate that was filtered and washed with cold water. The collected solid was dried under vacuum for one week to give a yellow powder (530 mg, 92%). <sup>1</sup>H NMR (400 MHz, D<sub>2</sub>O, pH 13):  $\delta$  = 2.91 (m, 9H; CH<sub>3</sub>), 2.97 (m, 6H; CH<sub>2</sub>), 3.51 (m, 6H; CH<sub>2</sub>), 3.52 (m, 4H; CH<sub>2</sub>), 6.43 (d, 3H; ArH), 8.02 (d, 3H; ArH), 8.23 (d, 3H; ArH), 9.04 ppm (d, 3H; ArH); IR (ATR):  $\tilde{\nu}$  = 3600–3150, 1637, 1602, cm<sup>-1</sup>; ESI-MS: *m/z*: calcd [M+H]<sup>+</sup>: 941.17; found: 942.20; elemental analysis calcd (%) for C<sub>39</sub>H<sub>39</sub>N<sub>7</sub>O<sub>15</sub>S<sub>3</sub>·2H<sub>2</sub>O: C 47.90, H 4.43, N 10.03; found: C 47.53, H 4.43, N 10.08.

**Physicochemical measurements:** Analytical-grade solvents and chemicals (Fluka AG) were used without further purification. HBS buffer was prepared by mixing a solution of 4-(2-hydroxyethyl)piperazine-*N'*-2-ethane-

sulfonic acid (HEPES, 10 mM) and a solution of NaCl (150 mM, in doubly distilled water). Stock solutions of lanthanides were prepared just before use in freshly boiled, doubly distilled water from the corresponding perchlorate salts Ln(ClO<sub>4</sub>)<sub>3</sub>·*n*H<sub>2</sub>O (Ln = La, Nd, Eu, Gd, Dy, Er, Yb, and Lu; *n* = 3–6). **Caution!** Perchlorate salts combined with organic ligands are potentially explosive and should be handled in small quantities and with adequate precautions.<sup>[26,27]</sup> These salts were prepared from their oxides (Rhône-Poulenc, 99.99%) in the usual way.<sup>[28]</sup> Concentrations of solutions were determined by performing complexometric titrations using a standardized Na<sub>2</sub>H<sub>2</sub>EDTA solution in urotropine-buffered medium and with xylenol orange as indicator.<sup>[29]</sup> UV/Vis absorption spectra were measured by using a Perkin–Elmer Lambda 900 spectrometer with quartz Suprasil cells of 0.2- and 1-cm path length.

**Spectrophotometric titrations:** Spectrophotometric titrations were performed by using a J & M diode array spectrometer (Tidas series) connected to an external computer. All titrations were performed in a thermostated (25.0  $\pm$  0.1°C) glass-jacketed vessel at  $\mu$  = 0.1 M (KCl). In a typical experiment, a ligand solution (50 mL, 6.5  $\cdot$  10<sup>-6</sup> M) was titrated with freshly prepared sodium hydroxide solutions at different concentrations (4, 1, 0.1, and 0.01 M). After each addition of base, the pH of the solution was measured by a KCl-saturated electrode and the UV/Vis absorption spectrum was recorded by using a 1-cm Hellma optrode immersed in the thermostated titration vessel and connected to the Tidas spectrometer. By using the same equipment, conditional stability constants were determined by titration of **T2soxMe** by Ln<sup>III</sup> at fixed pH (0.1 M HBS buffer, pH 7.4). Factor analysis<sup>[30]</sup> and mathematical treatment of the spectrophotometric data were performed by using the SPECFIT program.<sup>[31,32]</sup>

**Potentiometric titrations: T2soxMe** (H<sub>7</sub>L)<sup>+</sup> was titrated by using a 5 mL sample ([H<sub>7</sub>L<sup>+</sup>]<sub>tot</sub> = 5.98  $\cdot$  10<sup>-4</sup> M in H<sub>2</sub>O) in a thermostated (25.0  $\pm$  0.1°C) glass-jacketed vessel under Ar atmosphere. The ionic strength was fixed with KCl ( $\mu$  = 0.1 M). The solution was acidified to pH  $\sim$  2.0 with 37% HCl 30 min before titration. Titrations were carried out by using an automatic Metrohm Titrimo 736 GP potentiometer (resolution 0.1 mV, accuracy 0.2 mV) linked to an IBM PS/2 computer and by using constant volume addition (0.025 mL). An automatic burette (Metrohm 6.3013.210, 10 mL, accuracy 0.03 mL) was used along with a Metrohm 6.0238.000 glass electrode. The standard base solution (NaOH 0.1 M) was added inside the solution through a capillary tip attached to the automatic burette. The data (200 points, drift  $<$  1 mV min<sup>-1</sup>) were mathematically treated by the program HYPERQUAD2000<sup>[33]</sup> by using a Marquardt algorithm, and the distribution of species was calculated by using the program HYSS2. Calibration of the pH meter and the electrode system was performed prior to each measurement by using a standardized HCl solution at 25.0°C: 10 mL of the latter was titrated with a standardized 0.1 M NaOH solution, and the electrode potential readings were converted to pH values. The ion product of water ( $pK_w$  = 13.91) and electrode potential were refined by using the program Scientist by Micromath (Version 2.0).

**Luminescence measurements:** Low-resolution luminescence measurements (spectra and lifetimes) were recorded by using a Fluorolog FL 3-22 spectrometer from Spex-Jobin-Yvon-Horiba with double-grating emission and excitation monochromators, and a R928P photomultiplier. For measurements in the NIR spectral range, the spectrometer was fitted with a second measuring channel equipped with a FL-1004 single-grating monochromator and light intensity was measured by two Jobin–Yvon solid-state InGaAs detectors 1) DSS-IGA020L, cooled to 77 K (range 800–1600 nm) and 2) DSS-IGA020A (range 800–1700 nm) working at RT and inserted into an LN2 housing including an elliptical mirror (90° beam path) and coupled to a Jobin–Yvon SpectraAcq2 data acquisition system. The equipment and experimental procedures for luminescence measurements in the visible and NIR ranges have been published previously.<sup>[13]</sup> All spectra were corrected for the instrumental functions. Phosphorescence lifetimes were measured in frozen glycerol/water solutions (10:90%) in time-resolved mode. They are averages of three independent measurements that were taken by monitoring the decay at the maxima of the emission spectra, enforcing a 0.05–0.5 ms delay. The monoexponential decays were analyzed by using the package Origin 7.0. Quantum yields of the complexes at pH 7.4 (HBS buffer) and at RT were determined rela-

tive to  $[\text{Yb}(\text{tta})_3(\text{H}_2\text{O})_2]$  (TTA = thenoyltrifluoroacetylacetonate) in toluene,  $Q_{\text{Yb}}^{\text{L}} = 0.35\%$ <sup>[34]</sup> for the NIR-emitting complexes. The estimated error is  $\pm 10\%$ . Quartz Suprasil cells with 0.2-cm path length were used for these measurements.

**Cell culture and complex loading:** The influence of the Yb-T2soxMe complex (1 mM in HBS) on cell viability was tested by using the human T leukaemia cell line Jurkat (ATCC TIB152). The cells were cultivated in 75 cm<sup>2</sup> tissue-culture flasks by using RPMI 1640 supplemented with 10% foetal calf serum, 2 mM L-glutamine, 1 mM sodium pyruvate, 1% nonessential amino acids, and 1% HEPES (all from Gibco Cell Culture, Invitrogen, Basel, Switzerland). Cultures were maintained at 37°C under 5% CO<sub>2</sub> and 95% air atmosphere. The growth medium was changed every other day until the cells were ready for use. Cell density and viability (defined as the ratio of the number of viable cells to the total number of cells) of the cultures were determined by using trypan-blue staining and a Neubauer improved hemacytometer (Blau Brand, Wertheim, Germany). Prior to each viability test, the cells were harvested and diluted at a density of  $7.5 \cdot 10^5$  cells mL<sup>-1</sup>. The cell suspension was seeded into 96-well plates at 100  $\mu\text{L}$ /well 2 h prior to addition of the Yb-T2soxMe complex and WST-1 reagent.

**Cytotoxicity tests:** The effect of incubation time for cell survival in the WST-1 test was evaluated by performing tests from 0.5 to 24 h (0.5, 1, 2, 3.5, 4.5, and 24 h). The WST-1 (Cell Proliferation Reagent WST-1, Roche, Germany) is a slightly red tetrazolium salt that is reduced only in living, metabolically active cell mitochondria.<sup>[35,36]</sup> After reduction (Figure 8), a dark-red formazan dye was formed and the number of living

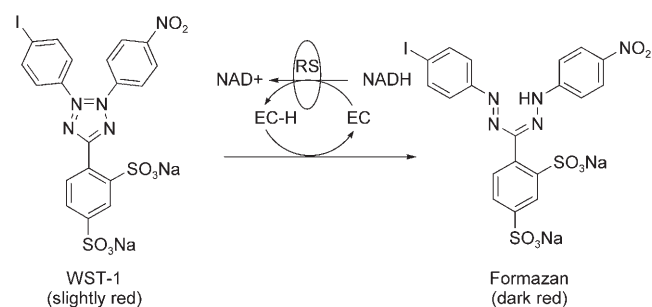


Figure 8. Cleavage of the tetrazolium salt (WST-1) to formazan (EC = electron coupling reagent, RS = mitochondrial succinate/tetrazolium/reductase system).

cells could be quantified spectrophotometrically. The test was performed as follows: Cells were seeded in a 96-well tissue-culture microplate at a concentration of  $7.5 \cdot 10^4$  cells/well in 100  $\mu\text{L}$  of a culture medium and incubated for 2 h at 37°C with 5% of CO<sub>2</sub>. The Yb-T2soxMe complex was dissolved at a concentration of 1 mM in fresh HBS at RT, and 100  $\mu\text{L}$  was added to each well (final concentrations: 500, 250, 125, and 50  $\mu\text{M}$ ); 20  $\mu\text{L}$  of the WST-1 reagent was added to each well and the plate was shaken for 1 min on a microtiter-plate shaker (450 rpm). The plate was further incubated at 37°C with 5% of CO<sub>2</sub> and the absorbance of the formazan product was measured at 450 nm. Cell viability was calculated from the absorbance values as follows:

$$\text{viability}_{\text{WST}} [\%] = \frac{(A_{450 \text{ nm}} - A_{650 \text{ nm}})_{\text{exp}}}{(A_{450 \text{ nm}} - A_{650 \text{ nm}})_{\text{medium}}} \times 100 \quad (7)$$

in which  $A_{450 \text{ nm}} - A_{650 \text{ nm}}$  is the difference in absorption at 450 and 650 nm for the cells that were in contact with the Yb-T2soxMe complex ("exp") and for the "medium" containing the Yb-T2soxMe complex at different concentrations. The results are expressed as an average over eight nominally identical measurements.

## Acknowledgements

This research was supported through grants from the Swiss National Science Foundation. We thank Mr. Frédéric Gummy for his help with the luminescence measurements.

- [1] R. Weissleder, V. Ntziachristos, *Nat. Med.* **2003**, *9*, 123–128.
- [2] S. Faulkner, S. J. A. Pope, B. P. Burton-Pye, *Appl. Spectrosc. Rev.* **2005**, *40*, 1–31.
- [3] S. Comby, J.-C. G. Bünzli, "Lanthanide Near-Infrared Luminescence in Molecular Probes and Devices", *Handbook on the Physics and Chemistry of Rare Earths, Vol. 37* (Eds.: K. A. Gschneidner, Jr., J.-C. G. Bünzli, V. K. Pecharsky), Elsevier, Amsterdam, in press.
- [4] Y. Hasegawa, Y. Wada, S. Yanagida, *J. Photochem. Photobiol. C* **2004**, *5*, 183–202.
- [5] J.-C. G. Bünzli, C. Piguet, *Chem. Soc. Rev.* **2005**, *34*, 1048–1077.
- [6] J.-C. G. Bünzli, *Acc. Chem. Res.* **2006**, *39*, 53–61.
- [7] J.-C. G. Bünzli, C. Piguet, *Chem. Rev.* **2002**, *102*, 1897–1928.
- [8] C. Piguet, J.-C. G. Bünzli, *Chem. Soc. Rev.* **1999**, *28*, 347–358.
- [9] D. E. Koshland, Jr., *Angew. Chem.* **1994**, *106*, 2468–2472; *Angew. Chem. Int. Ed. Engl.* **1994**, *33*, 2375–2378.
- [10] C. Reinhard, H. U. Güdel, *Inorg. Chem.* **2002**, *41*, 1048–1055.
- [11] W. D. Horrocks, Jr., J. P. Bolender, W. D. Smith, R. M. Supkowski, *J. Am. Chem. Soc.* **1997**, *119*, 5972–5973.
- [12] R. Ziessel, G. Ulrich, L. J. Charbonnière, D. Imbert, R. Scopelliti, J.-C. G. Bünzli, *Chem. Eur. J.* **2006**, *12*, 5060–5067.
- [13] S. Comby, D. Imbert, A.-S. Chauvin, J.-C. G. Bünzli, *Inorg. Chem.* **2006**, *45*, 732–743.
- [14] H. Schmidt, C. Lensink, S. K. Xi, J. G. Verkade, *Z. Anorg. Allg. Chem.* **1989**, *578*, 75–80.
- [15] W. D. Shrader, J. Celebuski, S. J. Kline, D. Johnson, *Tetrahedron Lett.* **1988**, *29*, 1351–1354.
- [16] G. Serratrice, H. Boukhalfa, C. Beguin, P. Baret, C. Caris, J. L. Pierre, *Inorg. Chem.* **1997**, *36*, 3898–3910.
- [17] A. E. Martell, R. M. Smith, *Critical Stability Constants*, Plenum Press, New York, **1974**.
- [18] C. Platas, F. Avecilla, A. de Blas, T. Rodriguez-Blas, C. F. G. C. Geraldes, E. Tóth, A. E. Merbach, J.-C. G. Bünzli, *J. Chem. Soc. Dalton Trans.* **2000**, 611–618.
- [19] M. H. V. Werts, J. W. Verhoeven, J. W. Hofstraat, *J. Chem. Soc. Perkin Trans. 2* **2000**, 433–439.
- [20] S. Faulkner, A. Beeby, M.-C. Carrié, A. Dadabhoy, A. M. Kenwright, P. G. Sammes, *Inorg. Chem. Commun.* **2001**, *4*, 187–190.
- [21] A. Beeby, B. P. Burton-Pye, S. Faulkner, G. R. Motson, J. C. Jeffery, J. A. McCleverty, M. D. Ward, *J. Chem. Soc. Dalton Trans.* **2002**, 1923–1928.
- [22] A. Beeby, I. M. Clarkson, R. S. Dickins, S. Faulkner, D. Parker, L. Royle, A. S. de Sousa, J. A. G. Williams, M. Woods, *J. Chem. Soc. Perkin Trans. 2* **1999**, 493–503.
- [23] J. Hamblin, N. Abboyi, M. P. Lowe, *Chem. Commun.* **2005**, 657–659.
- [24] R. Van Deun, P. Fias, P. Nockemann, A. Schepers, T. N. Parac-Vogt, K. Van Hecke, L. Van Meervelt, K. Binnemans, *Inorg. Chem.* **2004**, *43*, 8461–8469.
- [25] D. D. Perrin, W. L. F. Armarego, *Purification of Laboratory Chemicals*, Pergamon Press, Oxford, **1988**.
- [26] W. C. Wolsey, *J. Chem. Educ.* **1973**, *50*, A335–A337.
- [27] K. N. Raymond, *Chem. Eng. News* **1983**, *61* (Dec. 5), 4.
- [28] J. F. Desreux, *Lanthanide Probes in Life, Chemical and Earth Sciences: Theory and Practice* (Eds.: J.-C. G. Bünzli, G. R. Choppin), Elsevier, Amsterdam, **1989**, pp. 43–64.
- [29] G. Schwarzenbach, *Complexometric Titrations*, Chapman & Hall, London, **1957**.
- [30] E. R. Malinowski, D. G. Howery, *Factor Analysis in Chemistry*, John Wiley, New York, Chichester, Brisbane, Toronto, **1991**.
- [31] H. Gampp, M. Maeder, C. J. Meyer, A. D. Zuberbühler, *Talanta* **1985**, *32*, 257–264.
- [32] H. Gampp, M. Maeder, C. J. Meyer, A. D. Zuberbühler, *Talanta* **1986**, *33*, 943–951.



- [33] L. Alderighi, P. Gans, A. Ienco, D. C. Peters, A. Sabatini, A. Vacca, *Coord. Chem. Rev.* **1999**, 311–318.
- [34] S. B. Meshkova, Z. M. Topilova, D. V. Bolshoi, S. V. Beltyukova, M. P. Tsvirko, V. Y. Venchikov, *Acta Phys. Pol. A* **1999**, 95, 983–990.
- [35] M. Ishiyama, M. Shiga, K. Sasamoto, M. Mizoguchi, P. G. He, *Chem. Pharm. Bull.* **1993**, 41, 1118–1122.
- [36] M. Ishiyama, K. Sasamoto, M. Shiga, Y. Ohkura, K. Ueno, K. Nishiyama, I. Taniguchi, *Analyst* **1995**, 120, 113–116.

Received: July 6, 2006  
Published online: October 31, 2006